buildings

MDPI

Article

Experimental and Numerical Investigation of Airflow Organization in Modular Data Centres Utilizing Floor Grid Air Supply

Jingping Zhao, Jianlin Wu * and Mengying Li

China Academy of Building Research Ltd., Beijing 100013, China; zhaojingping1115@foxmail.com (J.Z.); mengying5353@gmail.com (M.L.)
* Correspondence: wujianlin@chinaibee.com

Abstract: Under the background of "dual carbon" development goals, the rapid expansion of internet data centers driven by advancements in 5G technology has led to increased energy consumption and elevated heat densities within the server rooms in these facilities. In this study, the modular data center is taken as the research object for the purpose of figuring out a way to improve the thermal environment of the computer room, reduce power consumption, and ensure the safe and stable running of servers. To this end, this study established an airflow organization model for the modular data center and verified this model through experimental methods. Computational Fluid Dynamics (CFD) simulations were employed to investigate the effects of raised floor height, floor opening rate, and cold/hot air channel closure on airflow organization. Furthermore, the efficiency of airflow organization was evaluated using entransy loss metrics. The results show that optimal airflow conditions are achieved when the height of the raised floor is 600–800 mm, the opening rate is 40%, and the combined opening is 40%. Additionally, the closure of either the cold channel or both the cold and hot channels significantly improves airflow performance. Specifically, cold channel closure is recommended for new data centers with underfloor air supply systems, while combined cold and hot channel closure is suitable for data centers with high power density and extended air supply distances.

Keywords: floor grille; data center; airflow organization; entransy loss

check for updates

Citation: Zhao, J.; Wu, J.; Li, M. Experimental and Numerical Investigation of Airflow Organization in Modular Data Centres Utilizing Floor Grid Air Supply. *Buildings* **2024**, *14*, 2750. https://doi.org/10.3390/buildings14092750

Academic Editor: Zhenjun Ma

Received: 21 July 2024
Revised: 15 August 2024
Accepted: 24 August 2024
Published: 2 September 2024

Copyright: © 2024 by the authors. Licensee MDPI, Basel, Switzerland. This article is an open access article distributed under the terms and conditions of the Creative Commons Attribution (CC BY) license (https://creativecommons.org/licenses/by/4.0/).

1. Introduction

In the context of the rapid development of global informatization, big data has become a critical strategic resource for nations, leading to a new round of scientific and technological innovation and promoting economic transformation and development. The global data volume is projected to expand from 16.1 zettabytes in 2016 to 163 zettabytes (about 18 billion GB) by 2025, resulting in a sustained increase in the demand for data centers. Data centers, which are energy-intensive infrastructures, consume power at an average rate approximately 30 times higher than that of a standard office environment [1]. The rapid development of cloud computing, big data, artificial intelligence, blockchain, 5G, and other information technologies is contributing to the burgeoning scale of internet data center facilities. As the scale and number of data centers continue to grow, so does their energy consumption and heat density, posing significant economic and environmental challenges. Ensuring efficient thermal and energy management within data centers while maintaining the safe operation of IT equipment has thus become a focal point of industry concern. At present, the refrigeration and air conditioning systems serve as the major tools to provide cooling capacity for data center equipment, and their energy consumption accounts for 45% of the total energy consumption of data centers [2,3]. The high heat output of server equipment and the mixing of cold and hot air within the data center contribute to a thermal environment that often fails to meet operational requirements. This is typically addressed

by increasing the supply air volume or reducing the supply air temperature. However, improper airflow organization in data centers is a primary cause of localized overheating of server equipment during operation [4]. The traditional approach of mitigating localized hot spots by lowering the temperature settings for the entire data center results in substantial energy waste. Therefore, optimizing airflow organization within data centers represents an effective strategy for enhancing the thermal environment, reducing overall energy consumption, and ensuring the stable and safe operation of server equipment.

In response to prevalent issues of localized overheating within data center rooms and cabinets caused by disorganized airflow, researchers have employed CFD software, such as Fluent, 6SigmsDC, and Flovent, to model and analyze airflow patterns and thermal conditions. Schmidt et al. [5] investigated the effects of variables such as cabinet heat dissipation, airflow volume, air conditioner positioning, and room height on cabinet inlet temperatures. Patankar et al. [6] identified significant impacts of raised floor height and floor grid layout on airflow organization within the data center rooms. Rajagopalan et al. [7] examined the influence of closed channels on airflow patterns in computer rooms, demonstrating that such channels enhance airflow mixing, with closed cold channels proving more efficient in cooling capacity utilization compared to closed hot channels, thereby promoting a more rational airflow arrangement. Gao et al. [8] used CFD to evaluate how the closure of cold channels affects cooling performance in computer rooms, finding that, when maintaining an adequate thermal environment, closed cold channels substantially improve cooling efficiency and raise the air supply temperature by 3 °C. Cho et al. [9] simulated the effects of air supply temperature of air conditioners and the configuration of closed hot and cold channels on the airflow organization within data centers. Their simulations revealed that the air supply temperature of air conditioners had the greatest impact on airflow organization of the computer room. Specifically, when the cold and hot channels were closed, the cabinet air supply temperature increased from 18 °C to 22 °C. Schmidr et al. [10] employed Fluent to simulate the exhaust temperature of racks under various isolation and closure schemes. Their findings indicated that adopting a cold channel containment strategy effectively facilitated comprehensive cooling of the equipment within the cabinets and led to a reduction in energy consumption. Shrivastava et al. [11] analyzed the effects of different air supply modes on airflow organization and temperature distribution within computer rooms. Their simulations demonstrated that implementing underfloor air supply combined with return air through a suspended ceiling successfully mitigated localized overheating issues in the data center. Nakao et al. [12] investigated the effects of various air supply modes on airflow distribution within data center rooms through simulation. Their findings indicated that optimal conditions, characterized by minimal air volume and supply temperature, were achieved when the return air was positioned at the top of the supply air under the rack. Fulpagare et al. [13] examined how obstacles, such as cables and pipelines, and the floor opening rate influenced airflow distribution beneath raised floors in computer rooms. Their simulations revealed that these obstacles could obstruct up to 80% of airflow from entering the cold channel, thereby increasing the incidence of hot spots within the computer room. Frankim et al. [14] utilized Flovent software to analyze the impact of obstacle placement beneath the floor and the opening rate of porous bricks on airflow uniformity and thermal conditions in data centers. Their results demonstrated that airflow uniformity was improved when cable slots and obstacles were positioned under the hot channel. Additionally, a 25% opening rate for porous bricks yielded better performance compared to opening rates of 50%, 75%, and 100%. The layout of cabinets in computer rooms significantly affects airflow recirculation, while the arrangement of air conditioners influences temperature distribution both across the array and within individual cabinets. Schmidt et al. [15] simulated the effects of varying the number of air conditioners and the configuration of floor grilles on outlet airflow and open floor rate. Their results showed that both the number of air conditioners and the floor grille configuration influenced airflow distribution. In cases where the airflow rate in the static pressure chamber was excessively high, reverse flow at the outlets was observed.

Fulpagare et al. [16] employed several metrics—including the rack cooling index (RCI), supply heat index (SHI), coefficient of performance (COP), and energy use efficiency (PUE)—to evaluate the uniformity of airflow organization and temperature within computer rooms. Their analysis indicated that a floor grille opening rate of 50% provided the most optimal airflow and temperature uniformity within acceptable evaluation ranges. This configuration also led to a reduction in air conditioning power consumption and an improvement in the overall system COP. Sharma et al. [17] introduced the supply heat index (SHI) and the regenerative index (RHI) for evaluating the thermal environment of computer rooms, aiding in thermal design and performance assessment. Herrlin et al. [18] proposed the return air temperature index (RTI) and the rack cooling index (RCI) to evaluate both the thermal environment and the efficiency of cooling systems within data centers. These indices were used to assess local airflow and cooling performance at the rack level. Nada et al. [19] utilized the heating index, reheating index, rewind temperature index, and rack cooling index to predict and evaluate temperature distribution and thermal conditions within data center racks. Their study analyzed the effectiveness of thermal management strategies based on these evaluation results. Qian et al. [20] employed two distinct evaluation metrics—entransy dissipation and entransy—to analyze airflow organization in server rooms. Their findings suggested that entransy dissipation analysis was more applicable than entranpy analysis, as it better reflected the utilization of cold capacity and the thermal environment within the server room.

To summarize, previous research has extensively simulated the airflow dynamics and thermal environment within data center rooms, investigating various aspects such as air return layouts for air conditioning systems, the impact of closed or open cold and hot channels, obstructions on raised floors, and the influence of opening rates on airflow patterns. Evaluation methods for air distribution in data center computer rooms have been proposed, including metrics such as RCI, SHI, COP, PUE, RTI, RHI, and entransy loss. Despite these advancements, the optimization of air distribution, particularly with respect to floor grid air supply, remains complex and warrants further investigation. Aiming at the above problems, this study focuses on a modular data center room, aiming to develop and validate an airflow organization model through experimental verification. The research efforts in this study involve the utilization of CFD simulations to analyze the effects of floor height, floor opening rate, and the closure of cold/hot air ducts on airflow patterns. Additionally, this study evaluates the airflow organization within the data center using the entransy loss method to provide a comprehensive assessment. By analyzing the entransy loss analysis of the data center, the mixing degree of cold and hot airflow in various airflow organization forms can be clarified, which provides a theoretical basis for the design of the data centers.

2. Materials and Methods

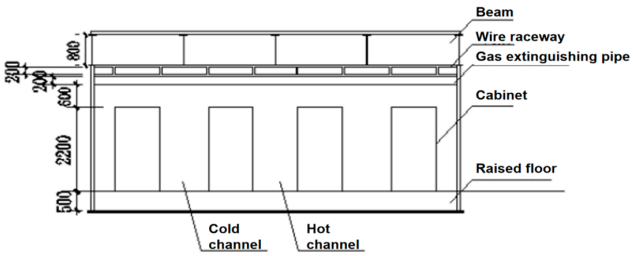
In this section, the thermal principles underlying entransy loss are applied to assess air distribution within data centers. A standardized data center model is constructed using 6SigmaDC with CFD simulation software to facilitate a comprehensive simulation analysis.

2.1. Experiment

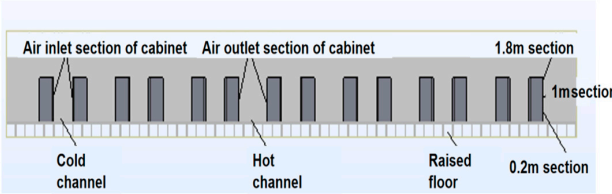
2.1.1. Experimental Subjects

Figure 1a,b illustrate a single-module computer room with a floor area of 427.68 m^2 (26.4 m × 16.2 m) and an overall height of 4.5 m. The room is equipped with 160 standard 42U cabinets arranged in a configuration of 10 columns by 16 rows. Each cabinet measures 600 mm in width, 1200 mm in depth, and 50 mm in height. The raised floor has a design height of 600 mm, with floor grilles measuring 600 mm × 600 mm, and an opening ratio of 40%. The cooling system in the computer room utilizes an underfloor air supply mode. In this system, cold air generated by the air conditioning units is directed into the plenum beneath the raised floor. This air is then distributed through the grilles to cool the servers within the cabinets. Additionally, the computer room features two return air ports,

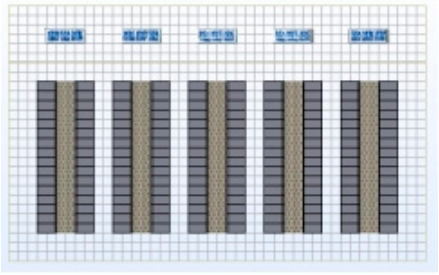
each measuring 1000 mm × 1000 mm, located on the inner wall of the air conditioning compartment. The height of the raised floor is 0.5 m, resulting in a vertical distance of 3.3 m between the raised floor and the ceiling. In Figure 1c,d, five special air conditioners with a sensible cooling capacity of 140 kW and air volume of 44,600 m^3/h are selected and arranged in the air conditioning compartment. The cooling mode of the cabinet server is that the air conditioning unit is supplied to the floor static pressure box and then sent to the cold channel through the floor grille to cool the server in the cabinet. The design value of the raised floor height is 600 mm, the floor grille size is 600 mm (length) and 600 mm (width), and the floor grille opening rate is 40%. A cold/hot aisle is set up; the width of the cold aisle is 1.2 m, the width of the hot aisle is 1.2 m, and the data center is organized by the air supply airflow under the overhead floor, and the plane view (c) and three-dimensional view (d) of the equipment layout of the computer room are shown in Figure 1c,d. Figure 2 presents the schematic diagram of the air distribution system. Figure 3 includes schematic diagrams depicting a single-cabinet configuration, the raised floor, and side airflow patterns.



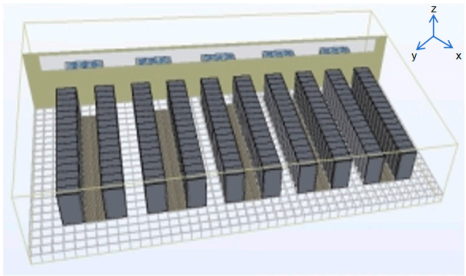
(**a**) Elevation of data centers



(**b**) Cabinet layout of data centers



(**c**) Plane view of data centers



(**d**) Three-dimensional view of data centers

Figure 1. Single-module data centers.

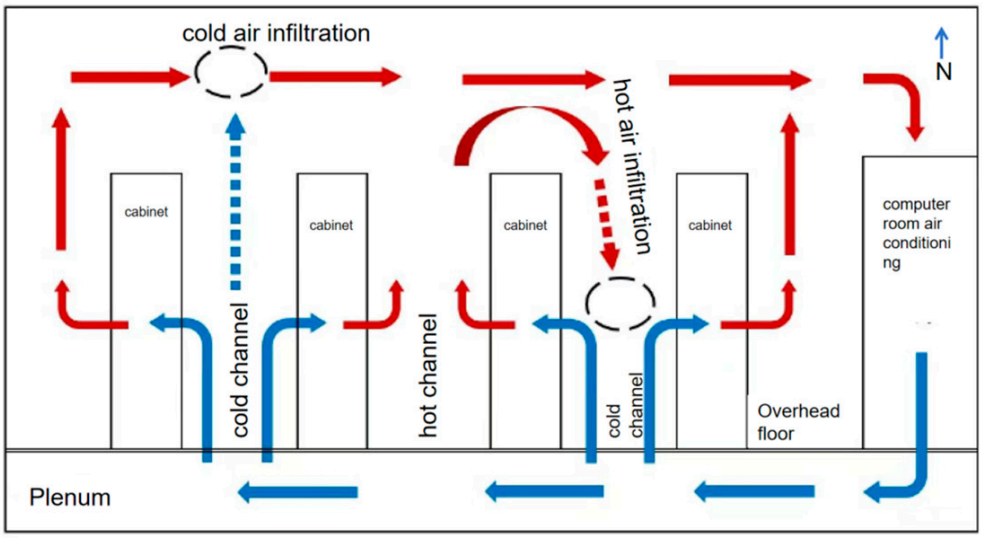
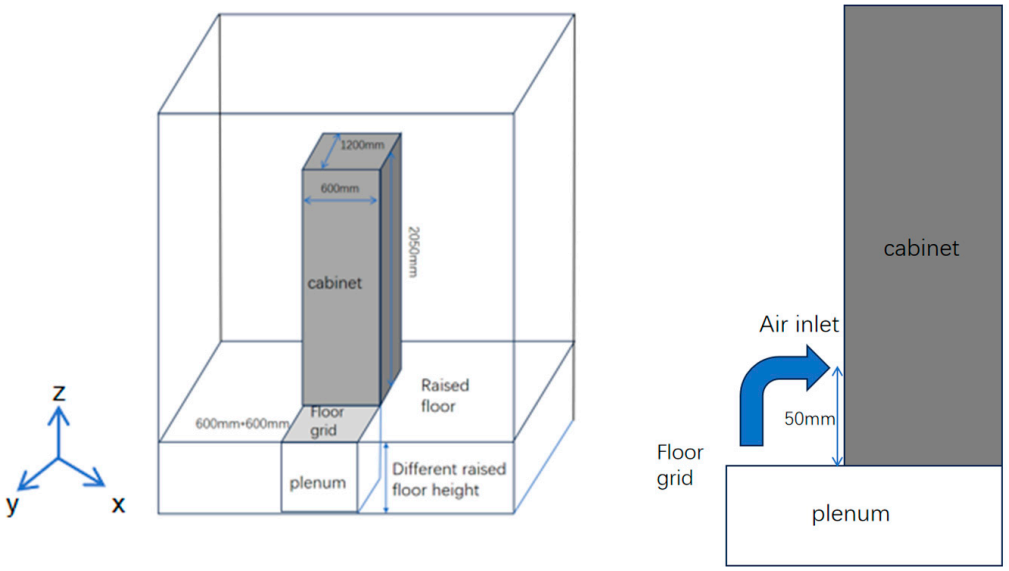


Figure 2. Schematic diagram of the airflow organization in the data centers.



(**a**) Geometry of a Single Cabinet (**b**) Side view of a Cabinet

Figure 3. The schematic diagram of a single cabinet.

2.1.2. Experimental Test

The temperature and wind speed were measured at the return air ports in the computer room. The floor grille, with dimensions of 600 mm × 600 mm, was subdivided into four equal areas. Measurements of wind temperature and speed were conducted at the center of each subdivision. Similarly, the return air outlet was divided into four areas, with measurements taken at the centers of these subdivisions, as illustrated in Figure 4. To determine the average temperature, humidity, and speed of the floor grille air supply, the arithmetic mean of measurements from four points was calculated. Each measuring point was assessed three times to ensure accuracy. Measurement points at return airport 1 were numbered 1 through 9, while those at return airport 2 were numbered 10 through 18. The instruments used for testing included a temperature and humidity meter and a hot wire anemometer, both provided by Testo Instruments International Trade (Shanghai) Co., Ltd. (Shanghai, China). The performance parameters of these instruments are detailed in Table 1.

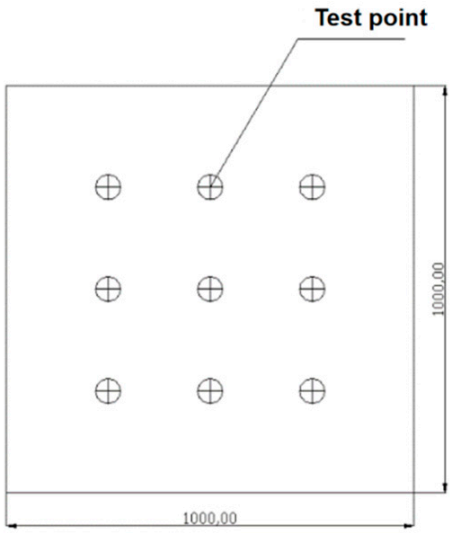


Figure 4. Layout of test room air return test points.

Table 1. Measurement parameters and instrumentation.

Testing Equipment	Measurement Parameter	Measuring Range	Precision
Hygrometer	Temperature	10~+60 °C	±2.5% RH
	humidness	0~+100%RH	±0.5 °C
Hot wire anemometer	Wind speed	0~20 m/s	±0.03 m/s + 5%

2.2. Model Building and Verification

2.2.1. Basic Assumptions

(1). The walls, doors, and windows of the computer room are assumed to be closed, creating a sealed environment.
(2). The server operates with stability, and its heat dissipation is considered the sole internal heat source within the system.
(3). Air is modelled as an ideal gas, with its physical properties treated as constant throughout the analysis. Indoor gas flow is regarded as an incompressible viscous fluid flow state [12].
(4). The temperature and volumetric flow rate of the air supplied by the air conditioner are maintained as constant.
(5). Cabinets are represented using simplified IT black box models to streamline the analysis.
(6). To simplify the modelling of airflow through the floor grid, this study employs the method proposed by Iyengar et al. [21]. Specifically, the airflow through the floor grid is approximated as a single, concentrated jet, conserving both mass and momentum by reducing the flow area.
(7). Server heat depends on the CPU type and usage; the actual use process server heat will also change over time; in order to simulate conveniently, this article sets the server for constant power.

2.2.2. Mathematical Model

The mass conservation model of cold airflow in data centers is given as below:

$$\frac{\partial \rho}{\partial t} + \frac{\partial (\rho u)}{\partial x} + \frac{\partial (\rho v)}{\partial y} + \frac{\partial (\rho w)}{\partial z} = 0 \quad (1)$$

The momentum conservation model of cold airflow in data centers can be expressed using the following equation:

$$\begin{array}{l} \frac{\partial(\rho v)}{\partial t} + div(\rho v u) = -\frac{\partial p}{\partial y} + \frac{\partial \tau_{xy}}{\partial x} + \frac{\partial \tau_{yy}}{\partial y} + \frac{\partial \tau_{zy}}{\partial z} + F_y \\ \frac{\partial(\rho w)}{\partial t} + div(\rho w u) = -\frac{\partial p}{\partial z} + \frac{\partial \tau_{xz}}{\partial x} + \frac{\partial \tau_{yz}}{\partial y} + \frac{\partial \tau_{zz}}{\partial z} + F_z \\ \frac{\partial(\rho u)}{\partial t} + div(\rho u u) = -\frac{\partial p}{\partial x} + \frac{\partial \tau_{xx}}{\partial x} + \frac{\partial \tau_{yx}}{\partial y} + \frac{\partial \tau_{zx}}{\partial z} + F_x \end{array} \quad (2)$$

The energy conservation model for cold airflow in data centers can be expressed as follows:

$$\frac{\partial(\rho T)}{\partial t} + div(\rho u T) = div(\frac{k}{cp} grad T) + S_T \quad (3)$$

The *k*-ε turbulence model for high Reynolds number cold airflow in a data center is given as below:

$$K = \frac{1}{2}(\overline{u'^2} + \overline{v'^2} + \overline{w'^2}) \quad (4)$$

$$\overline{u'^2}\varepsilon = \frac{\mu}{\rho}(\overline{\frac{\partial u_1'}{\partial x_k}})(\frac{\partial u_1'}{\partial x_k}) \quad (5)$$

The flow viscosity, denoted as μ_t, can be expressed in terms of k and ε:

$$\mu_t = C_\mu \rho K^2 / \varepsilon \quad (6)$$

where k denotes the turbulent pulsation kinetic energy per unit mass flow; ε represents the flow dissipation rate; C_μ is the empirical constant.

2.3. Grid Division and Verification

The simulation was conducted using 6SigmsDC in CFD simulation software. The k-ε turbulence model, along with the control volume method, was employed to solve the differential equations, while the SIMPLE algorithm was utilized for solving the velocity–pressure coupling equations. A porous step model was applied to the floor grid. The diffusion term was discretized using the central difference method, and the momentum and energy equations were discretized with a first-order upwind scheme. The boundary conditions included air supply as the flow inlet and return air as the pressure outlet. Convergence accuracy was controlled by monitoring the calibrated residuals, which converged to 1, indicating that the parameter values were stabilizing.

To ensure the accuracy of the simulation results, grid independence testing was performed. The 6SigmsDC software automatically generates high-quality grids based on intelligent partitioning of different computer room models. The model is divided into 560,000, 1,000,000, 1,295,000, 2,459,000, 4,838,000, 7,835,000, 6 sets of grids to calculate the RHI of the data room while keeping the equipment setting parameters of the data room unchanged. The simulation grid is divided into standard hexahedral structured grids, and the grids are refined in areas with large velocity fluctuations such as air supply and return ports, air supply holes, air inlet and air outlet of the cabinet, and areas with large temperature changes inside the cabinet. The curve of RHI as a function of the number of meshes is as shown in Figure 5. When the number of meshes is at more than 1,295,000, RHI is essentially independent of the number of meshes. Considering the accuracy and running time of the simulation, the final number of grids was set at 1,295,000.

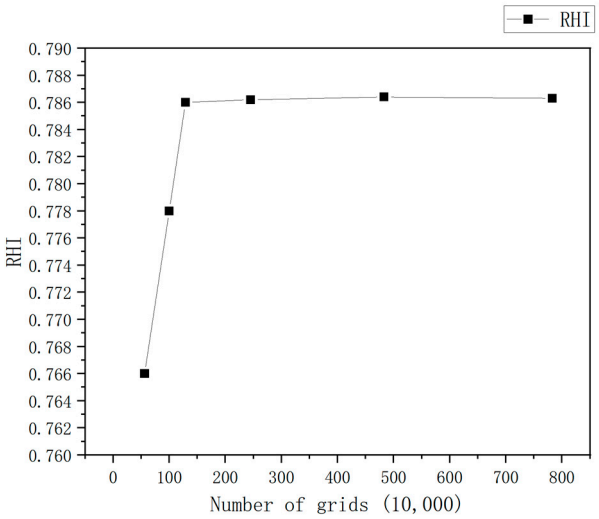


Figure 5. Grid independence verification.

2.4. Boundary Conditions and Operating Conditions

The air supply system employs first-type boundary conditions, with an air supply temperature set at 18 °C and relative humidity maintained at 50%. The return air outlet is configured with pressure outlet boundary conditions. The server power density is specified as 1.5 kW/m^2, while the standard heat dissipation capacity for an individual cabinet is 4 kW. Consequently, the total heat dissipation capacity for the entire cabinet reaches 640 kW. For the purposes of this study, the computer cabinets are modelled as exhibiting uniform thermal resistance across their entire cross-sectional area.

This study primarily investigates the effects of raised floor height, grille opening rates, and the switch between hot and cold channel configurations on airflow dynamics within the server room. The operating conditions are detailed in Table 2.

Table 2. Operating conditions.

Simulated Object	Operating Conditions
Raised floor	400–1000 mm
Floor grille	20–60%
Hot and cold channels	a Open cold/hot, b Open hot, c Open cold, d close cold/hot

2.5. Data Processing

Entransy is a physical quantity that describes the heat transfer capacity of an object relative to an absolute zero environment (0 K). For an object with a specific heat of c_p, a mass of m, and a traditional thermodynamic temperature of T, the heat product carried by it is defined as J_m (unit: W· K).

$$J_m = 1/2 c_p m T^2 \tag{7}$$

The thermal entransy of an object includes both temperature (thermal potential) and heat capacity, so the thermal entransy can be called the heat transfer potential, which is characterized by the maximum heat transfer capacity of the heat transfer system in the thermal potential field to transfer heat to the 0 K environment. For a stable-flow open system with several streams of fluid entering and exiting, the total heat transfer entransy loss of the system is equal to the sum of the thermal entransy of the inlet fluid minus the sum of the thermal entransy product carried by the outlet fluid, and the thermal entransy balance equation is as follows:

$$\Delta J_{loss} = \sum_i J_{in.i} - \sum_j J_{out,j} = \sum_n \Delta J_{loss,n} \tag{8}$$

The entransy balance equation reflects the change in the heat transfer capacity of the system during the heat transfer process, the entransy represents the quality of the energy transfer capacity, and the entransy loss represents the depreciation of the energy transfer quality.

The entransy loss J_{loss} during indoor mixing of hot and cold air in the data center is:

$$\begin{aligned} \Delta J_{loss} &= J_{a,input} - J_{a,output} \\ &= \left(\sum_i \tfrac{1}{2} C_{a,i} {T_{a,out,i}}^2 + \sum_i \tfrac{1}{2} C_{a,j} {T_{a,s,j}}^2 \right) - \left(\sum_i \tfrac{1}{2} C_{a,i} {T_{a,in,i}}^2 + \sum_i \tfrac{1}{2} C_{a,j} T_{a,r_1} \right) \end{aligned} \quad (9)$$

In the equation:
$C_{a,i}$—hot melt flow of the air inlet and exhaust of cabinet i;
$C_{a,j}$—the return air heat capacity flow of precision air conditioner j;
$T_{a,in,j}$—intake air temperature of cabinet i;
$T_{a,out,j}$—exhaust air temperature of cabinet i;
$T_{a,s,j}$—intake air temperature of precision air conditioner j;
$T_{a,r,j}$—exhaust air temperature of precision air conditioner j.

3. Results and Discussion

In this chapter, the air distribution methodology is assessed and analyzed using the thermal principle of entransy loss, with the aim of verifying the appropriateness of employing this evaluation method within data centers. The examination of data related to fire product loss analysis provides a theoretical foundation for the optimal design of data centers.

3.1. Model Verification

Table 3 presents a comparative analysis of the simulated and measured values of temperature and velocity at the return air outlet within the computer room. The findings of Return Air Inlet 1 indicate that the maximum relative error between the simulated temperature and the measured value is 15.19%, with an average relative error of 13.24%. Additionally, the maximum relative error for the simulated wind speed compared to the measured value is 15.10%, accompanied by an average relative error of 10.73%. In relation to Return Air Inlet 2, the maximum relative error between the simulated and measured values is 13.63%, while the average relative error stands at 7.73%. Furthermore, the assessment of wind speed at this inlet reveals a maximum relative error of 10.61% and an average relative error of 7.26%. Consequently, these results suggest that the model developed in this study demonstrates a satisfactory level of accuracy [8].

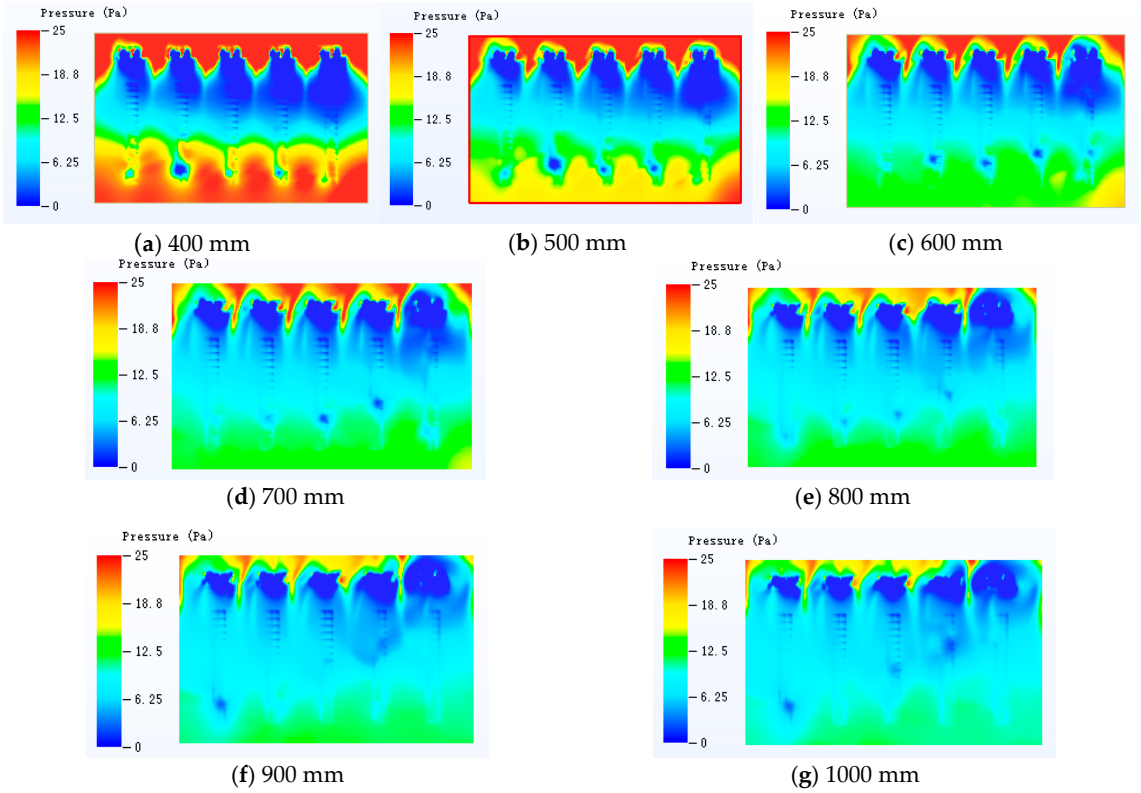
3.2. Effect of Raised Floor Height

The data center employs an underfloor air supply system, and the height of the raised floor impacts both the civil construction costs and the cooling efficiency of the servers. This study simulates the effects of various floor heights on the pressure field, velocity field, and temperature field. Figure 6 illustrates the pressure distribution at a horizontal section 200 mm below the floor grid for heights ranging from 400 mm to 1000 mm. To minimize pressure interference near the air supply outlet under the air conditioner, a pressure range of 5–25 Pa is considered as the effective measurement range. Figure 6a,b indicate that the pressure near the air conditioner is low, leading to reduced outlet air pressure and a diminished air volume through the floor grille. Conversely, higher pressure is observed at the remote end of the air conditioner, resulting in increased air discharge pressure and volume through the floor grille, causing an uneven pressure distribution along the cabinet's longitudinal direction. The relatively low air volume and average static pressure near the air conditioning units are primarily due to the perpendicular alignment of the cold airflow with the floor grille's wind direction. In the vicinity of the air conditioning units, the Bernoulli effect results in insufficient airflow through the floor grille due to the cold

air not passing through the adjacent air conditioning units but, rather, moving toward the far side of the unit. This leads to a reduced air volume through the floor grille near the air conditioning units and may even result in negative pressure backflow.

Table 3. Comparative analysis of return air temperature, speed analog values, and test measurements.

Measurement Points	Temperature			Velocity		
	Simulation Value /°C	Test Value /°C	Relative Error /%	Simulation Value /m/s	Test Value /m/s	Relative Error /%
1	27.1	23.8	13.87	2.82	2.54	11.02
2	27.1	24.2	11.98	3.1	2.72	13.97
3	27.3	23.7	15.19	3.43	2.98	15.10
4	26.7	24	11.25	2.74	2.56	7.03
5	27.4	23.9	14.64	2.98	2.72	9.56
6	27.4	23.8	15.13	3.43	2.98	15.10
7	26	23.5	10.64	2.66	2.52	5.56
8	26.3	23.5	11.91	2.91	2.71	7.38
9	27.5	24	14.58	3.31	2.96	11.82
Average value	26.98	23.82	13.24	3.04	2.74	10.73
10	26.9	23.9	12.55	3.44	3.11	10.61
11	26.9	24.3	10.70	3.46	3.14	10.19
12	26.8	24.1	11.20	3.38	3.32	1.81
13	26.7	23.5	13.62	3.41	3.22	5.90
14	25.8	24.4	5.74	3.33	3.04	9.54
15	24.9	23.8	4.62	3.3	3.11	6.11
16	25.8	24.3	6.17	3.15	2.95	6.78
17	24.2	23.8	1.68	3.01	2.82	6.74
18	23.5	24.3	3.29	2.81	2.61	7.76
Average value	25.72	24.04	7.73	3.25	2.98	7.26



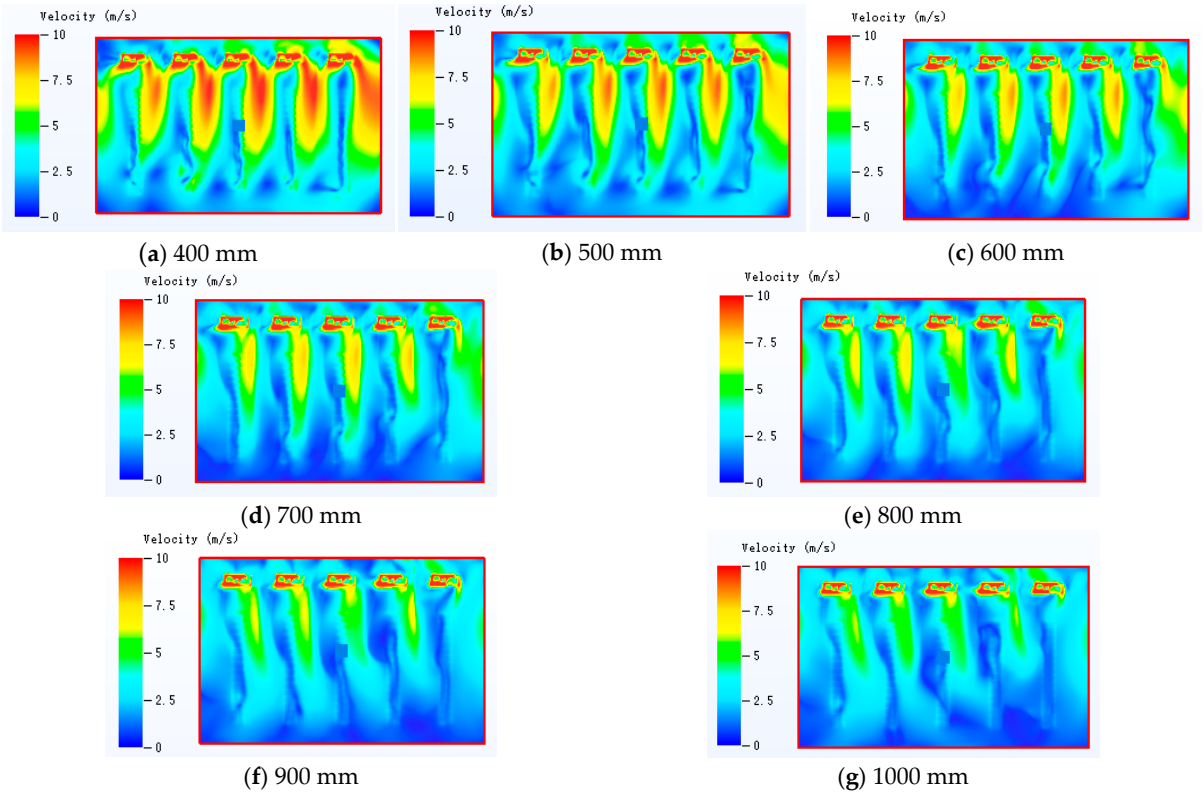
(**a**) 400 mm (**b**) 500 mm (**c**) 600 mm

(**d**) 700 mm (**e**) 800 mm

(**f**) 900 mm (**g**) 1000 mm

Figure 6. Pressure distribution beneath the raised floor.

Figure 7 illustrates the velocity distribution of a raised floor with a height ranging from 400 mm to 1000 mm, assessed at a horizontal section located 200 mm below the top surface. To mitigate interference from airflow near the air supply outlet of the air conditioning system, the effective velocity range is constrained between 0 and 10 m/s. Panels (a) to (g) of Figure 7 demonstrate that, as the height of the raised floor increases, the velocity distribution beneath the floor becomes more uniform, concurrently resulting in a reduction in the wind speed near the air conditioning outlet. This observation aligns with the principles outlined by the Bernoulli effect, which states that a decrease in dynamic pressure corresponds to an increase in static pressure. These findings are consistent with the data presented in Figure 6.



(**a**) 400 mm (**b**) 500 mm (**c**) 600 mm

(**d**) 700 mm (**e**) 800 mm

(**f**) 900 mm (**g**) 1000 mm

Figure 7. Velocity distribution beneath the raised floor.

Figure 8 illustrates the temperature distribution within a cabinet with varying raised floor heights, ranging from 400 mm to 1000 mm. The data indicate that an increase in the height of the raised floor corresponds to a decrease in the overall temperature within the equipment room. At a raised floor height of 400 mm, the temperature distribution in the computer room is highly uneven, resulting in suboptimal cooling performance. Specifically, the maximum temperature recorded at the air intake section of the cabinet reaches 30.5 °C, which significantly exceeds the recommended threshold of 27 °C. This discrepancy leads to uneven air distribution, with cold air failing to reach some cabinet entrances and warm air circulating back into the cold channel, thereby causing localized overheating. When the raised floor height is increased to 500 mm, there is a notable improvement in both the overall temperature reduction and the uniformity of temperature distribution within the computer room. Further increasing the raised floor height from 600 mm to 1000 mm results in a gradual decrease in cross-sectional temperature. The longitudinal temperature distribution across the cabinet becomes more uniform and the efficiency of the cooling system improves markedly. The enhanced height of the raised floor effectively reduces the static pressure variations within the floor plenum, facilitating more even distribution of cold air at the cabinet entrances and mitigating overheating at both ends of the cabinet channel.

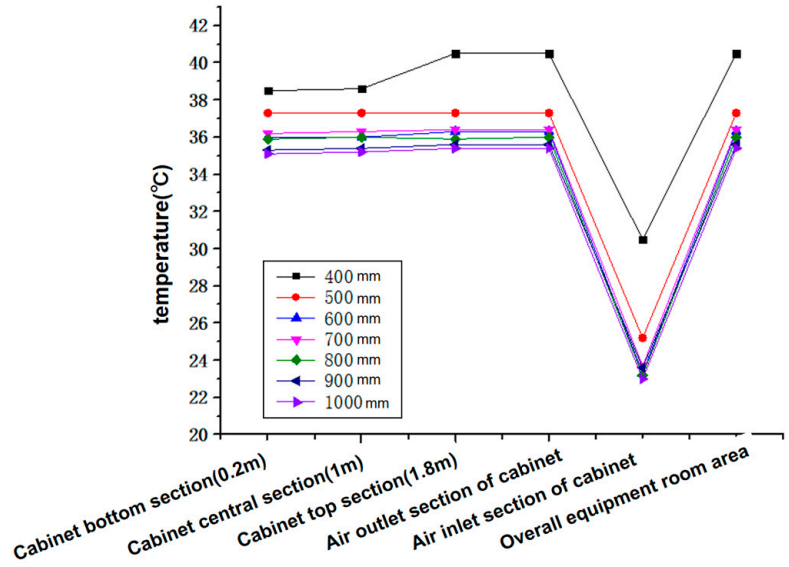


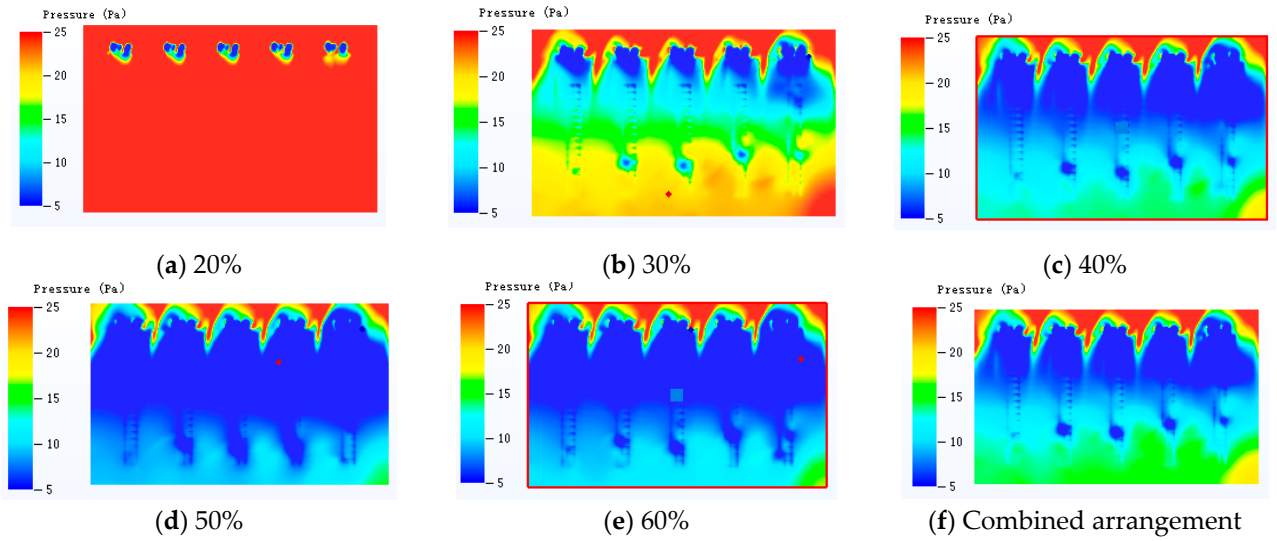
Figure 8. Variation in temperature of raised flooring at various elevations.

3.3. Effect of Floor Grille Opening Rate

The floor grille serves as the primary conduit for cold air entering the cabinet, and its opening rate has a direct impact on the cooling efficiency of the data center. This study investigates the effect of the floor grille's opening rate on the pressure field, velocity field, and temperature field within the server room. Figure 9 illustrates various opening rates of the floor grille, ranging from 20% to 60%, as well as different configuration types: 30% at the far end of the air conditioning zone, 40% in the middle of the channel, and 50% at the near end of the air conditioning zone, as depicted in Figure 10. The analysis focuses on the pressure distribution at a horizontal section located 200 mm from the top of the floor grille opening. In order to avoid the interference of too low or too high pressure near the air supply outlet under the air conditioner, to minimize the impact of pressure fluctuations near the air supply outlet under the air conditioner, the effective pressure range considered is between 5 and 25 Pa. As shown in Figure 9a, when the pressure in the static pressure chamber exceeds 25 Pa, the overall pressure is elevated, resulting in a reduced air discharge volume and higher air discharge velocity. This scenario causes the cold air entering the cabinet to bypass the intended areas, thereby decreasing cooling efficiency. Figure 9b indicates that the pressure in the static pressure chamber predominantly falls within the range of 10–20 Pa. Figure 9c,f show that the pressure distribution within the static pressure chamber averages around 10 Pa, with a relatively even distribution. Conversely, Figure 9d,e depict a pressure distribution in the plenum that is below 10 Pa, which signifies a high static pressure in the air supply area. Despite a high floor grille opening rate and substantial air output, the low static pressure in the plenum results in a reduced jet velocity of the cold air at the floor grille outlet. This insufficiency in cooling capacity within the cabinet, coupled with localized hot air recirculation, ultimately leads to diminished cooling efficiency within the data center.

Figure 11 illustrates the opening rates of the floor grille ranging from 20% to 60% and the corresponding speed distribution across the openings of the combined floor grille, measured at a horizontal section located 1800 mm above the floor. To eliminate interference from the airflow near the air supply outlet of the air conditioner, the effective measurement range is constrained to 0 to 10 m/s. In Figure 11a–f, it is observed that the uneven distribution of wind speed within the computer room diminishes as the opening rate of the floor grille decreases. Specifically, under the combined arrangement condition, the air volume corresponds to 30% to 40% of the floor grille's opening rate. When the opening rate varies from 20% to 60%, the wind speed near the grille outlet on the air conditioning side is relatively low, while the wind speed at the grille outlet farther from the air conditioning

side is higher. The combined grille arrangement effectively reduces the wind speed at the outlet of the floor grille located farthest from the air conditioner, while simultaneously increasing the wind speed at the outlets of the grille nearest to the air conditioner and at the middle grille within the cabinet channel.



(**a**) 20% (**b**) 30% (**c**) 40%

(**d**) 50% (**e**) 60% (**f**) Combined arrangement

Figure 9. Static pressure distribution under raised floor.

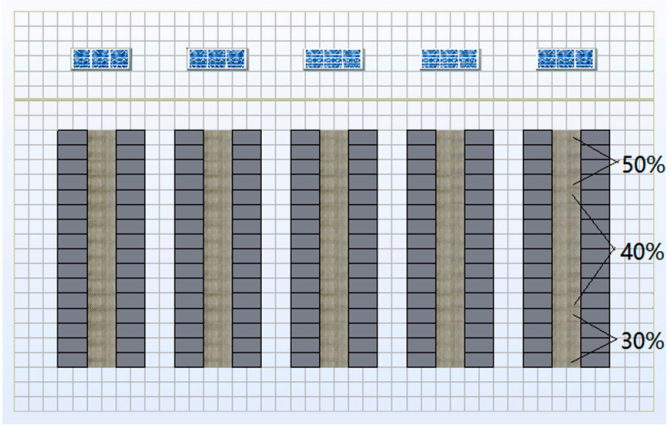


Figure 10. Combined openings of floor air supply grilles.

Figure 12 illustrates the temperature distribution in the vertical direction within the cabinet, considering varying opening rates of the floor grille, ranging from 20% to 60%, and the combined floor grille supply air. For opening rates between 20% and 40%, the temperature on each vertical plane decreases progressively with an increasing opening rate, leading to an enhanced cooling effect. Conversely, when the opening rate is between 50% and 60%, the temperature on each vertical plane exhibits a rising trend as the opening rate increases, resulting in a diminished cooling effect. Specifically, with floor grille opening rates of 20% or 60%, the temperature at the cabinet air intake section exceeds 27 °C, which fails to meet the design standard requirements. However, with an opening rate of 40%, the temperature at the air intake section is 23.3 °C, while the average temperature in the computer room is 36.3 °C, providing the most effective cooling performance.

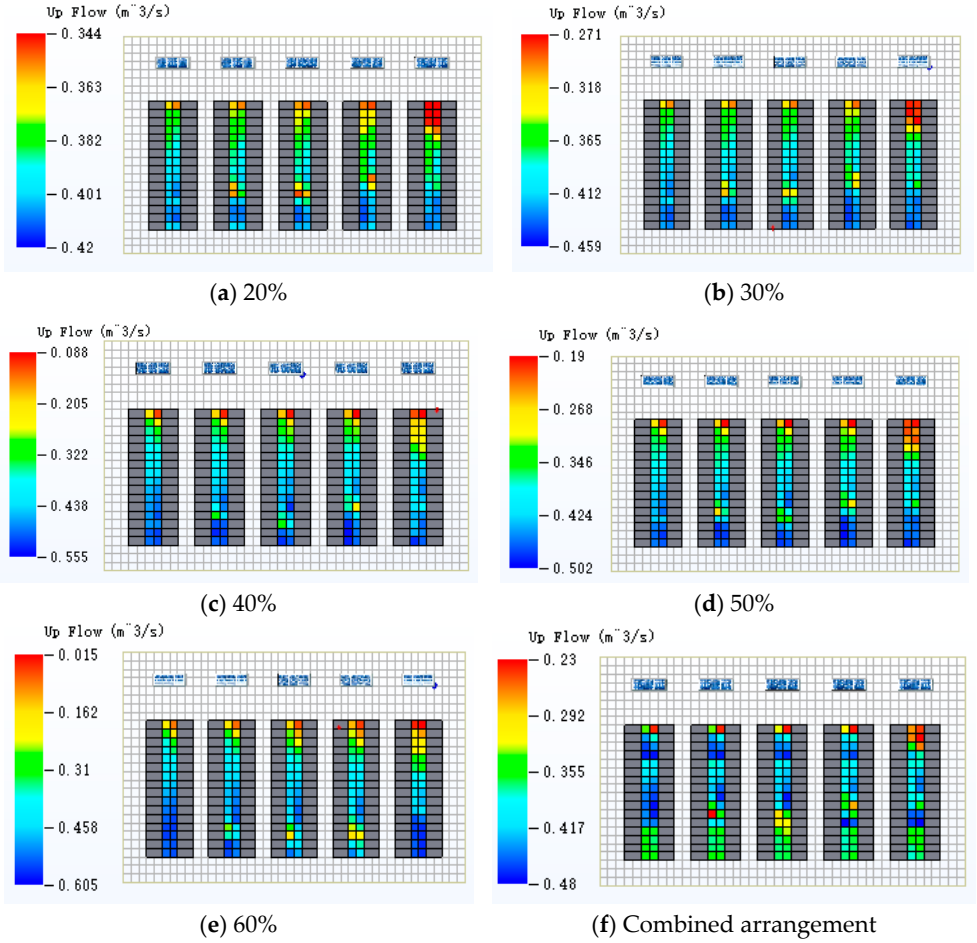


Figure 11. Speed distribution on the top of the cabinet.

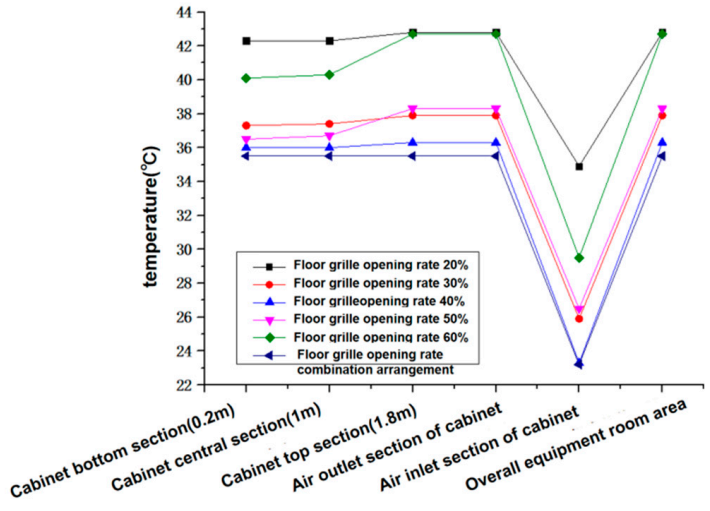


Figure 12. Vertical temperature distribution within the cabinet.

3.4. Effect of Closed Cold/Hot Channels

The implementation of cold/hot channel closures, as depicted in Figure 13, serves as an effective strategy to enhance cooling efficiency in data centers. The closure configurations between the cold and hot channels can be categorized into four operational conditions: simultaneous opening of both cold and hot channels, closure of the cold channel, closure of the hot channel, and simultaneous closure of both cold and hot channels. This study em-

ploys simulations to analyze the effects of various cold/hot channel closure configurations on the thermal field and airflow dynamics within the server room.

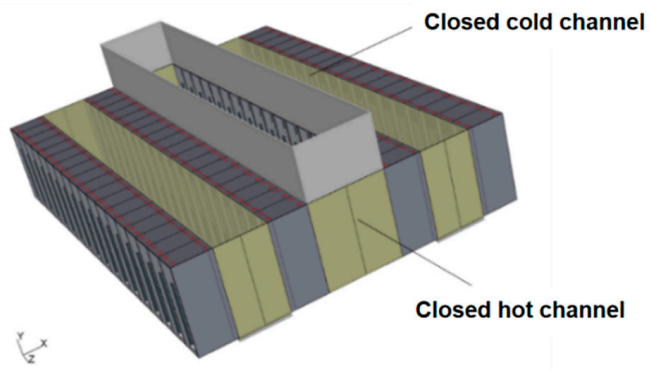


Figure 13. Diagram illustrating cold/hot channel closure.

Figure 14 illustrates the temperature distribution along the vertical axis of the cabinet under varying conditions of cold and hot channel closures. When both the cold and hot channels are open simultaneously, the maximum temperature at the cabinet air intake is 23.3 °C, while the maximum temperature at the cabinet exhaust is 36.3 °C. The simultaneous mixing of cold and hot air results in an increase in the intake temperature, which leads to localized overheating within the computer room and a substantial loss of cold air. This situation is detrimental to server performance, as depicted in Figure 14. When only the cold channel is closed, or only the hot channel is closed, or both channels are closed, the temperature at the cabinet interface is lower compared to when both channels are open. The overall temperature within the computer room decreases by approximately 7 °C, air distribution becomes more uniform, and the mixing of cold and hot air is significantly reduced. This isolation of cold and hot airflows enhances the efficiency of the cooling system. As illustrated in Figure 15, with the cold channel closed, the cold air that is not directed into the computer room passes through the hot channel. Conversely, when the hot channel is closed, the cabinet intakes cold air and expels hot air through the exhaust vents located at the top of the computer room. Consequently, the overall temperature in the computer room is reduced by 7.3 °C. If both the cold and hot channels are closed, the cabinet's air discharge temperature is 0.6 °C lower than when only the hot channel is closed.

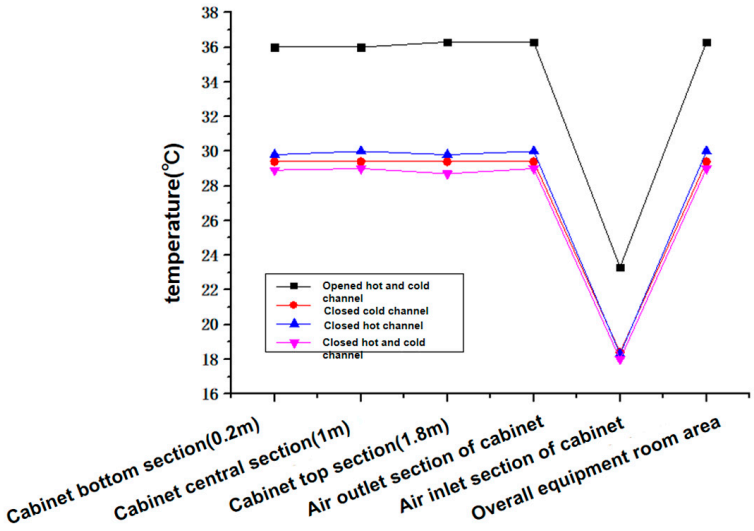
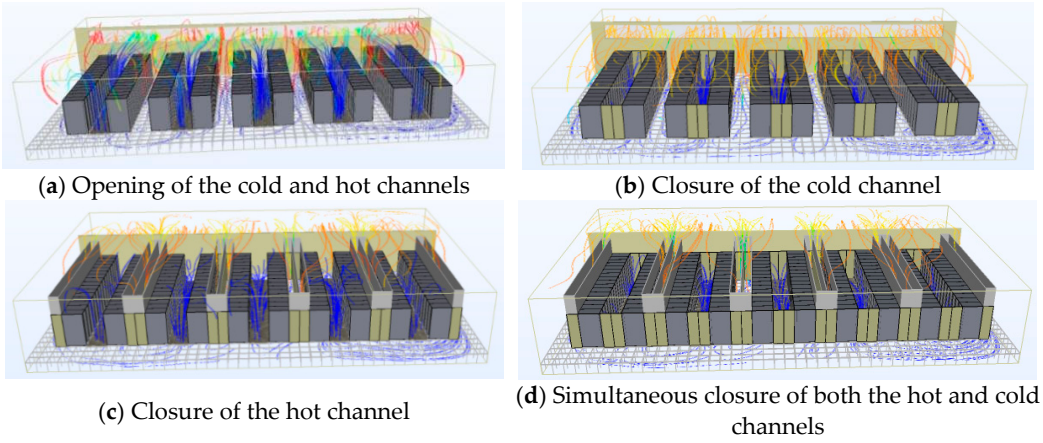


Figure 14. Temperature distribution within the enclosed cabinet's cold and hot channels.



(**a**) Opening of the cold and hot channels (**b**) Closure of the cold channel

(**c**) Closure of the hot channel (**d**) Simultaneous closure of both the hot and cold channels

Figure 15. Airflow organization in the server room.

3.5. Evaluation of the Entransy Loss in Airflow Tissue

Entransy loss is a critical metric for evaluating the mixing degree of hot and cold air within a data center, and it reflects the efficiency of cold air utilization. A higher entransy loss indicates a greater extent of mixing between hot and cold air, which, in turn, implies reduced efficiency in cooling the servers. Conversely, a lower entransy loss suggests a more effective utilization of cold air for server cooling. Figure 16 illustrates the entransy loss at various heights under the overhead floor. As the height increases from 400 mm to 500 mm, the entransy loss decreases significantly from 12,349.4 kW·K to 11,132.9 kW·K, indicating a notable reduction in air mixing. When the height is further increased from 500 mm to 800 mm, the entransy loss decreases marginally from 11,132.9 kW·K to 10,578.8 kW·K. At a height of 1000 mm, the entransy loss further decreases to 10,533.1 kW·K. However, raising the overhead floor height to 800 mm yields diminishing returns in reducing entransy loss. Considering both the reduction in entransy loss and the associated construction costs, an optimal overhead floor height range of 600–800 mm is recommended for balancing efficiency and cost.

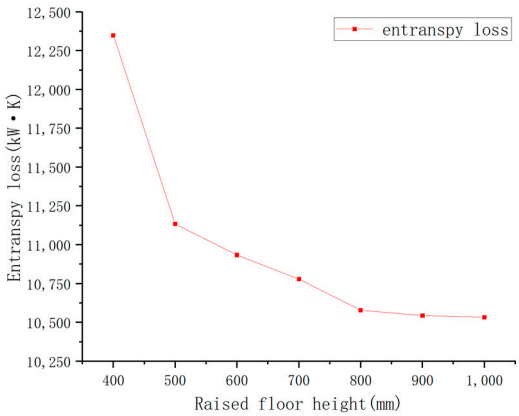


Figure 16. Energy loss due to entrapment at varying raised floor heights.

Figure 17 illustrates the relationship between entransy loss and various floor grid opening rates. As the opening rate increases from 20% to 40%, the entransy loss in the server room decreases from 16,642.0 kW·K to 10,933.8 kW·K. Conversely, when the opening rate rises from 40% to 60%, the entransy loss in the server room experiences an increase, escalating from 10,933.8 kW·K to 15,064.2 kW·K. At an opening rate of 40%, the mixing of cold and hot air within the server room is minimal, resulting in a high utilization rate of the cold air. Notably, when a combined opening configuration is employed, the entransy loss is recorded at 8238.3 kW·K, representing the lowest value observed. These findings

indicate that floor grids featuring combined opening holes achieve the least degree of cold and hot air mixing, thereby optimizing the utilization of cold capacity.

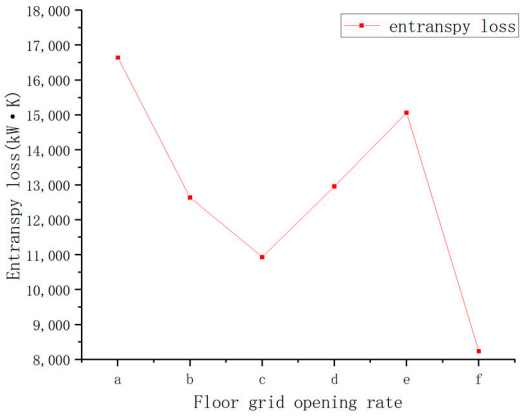


Figure 17. Entransy loss under different floor grid opening rates.

Figure 18 illustrates the entransy loss under varying conditions of closed cold and hot channels. When both cold and hot channels are simultaneously open, the entransy loss within the server room is measured at 16,500 kW·K. Conversely, with the closure of either cold or hot channels, the entransy loss is significantly reduced. Specifically, when both the cold and hot channels are closed simultaneously, the entransy loss in the room decreases to 3500 kW·K. The use of closed cold channels is particularly effective for computer rooms equipped with air supply systems positioned beneath a raised floor, as it mitigates the risk of cold and hot air mixing. On the other hand, the implementation of closed hot channels is advantageous for retrofitting older computer rooms that lack an elevated floor system. Although the overall entransy loss is minimal when both cold and hot channels are closed, this approach necessitates a high clear height within the computer room. Consequently, it entails a higher initial investment. This solution is most appropriate for computer rooms characterized by high power density and extensive air supply distances.

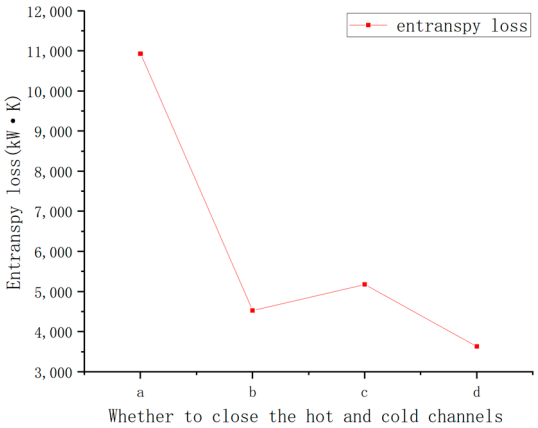


Figure 18. Entransy loss under closed cold/hot channel.

4. Conclusions

This study focuses on a module data center equipped with a 42U standard cabinet, with dimensions of 600 mm (width) × 1200 mm (depth) × 2050 mm (height). An air distribution model for the module data center was developed, and the model's accuracy was validated through experimental methods. This study employed CFD simulations to investigate the impact of raised floor height, floor opening ratio, and cold/hot air duct closure on air distribution. The entransy loss method was utilized to evaluate air distribution efficiency within the data center. The findings are summarized as follows:

(1) Raised Floor Height: Increasing the height of the raised floor leads to a reduction in dynamic pressure and an increase in static pressure underneath the floor, resulting in more stable airflow [6]. A higher raised floor height contributes to a more uniform speed distribution, lower wind speed near the air conditioning units, and a more even distribution of cold air at the cabinet entrance, thereby preventing overheating at the ends of the cabinet channel.

(2) Floor Opening Ratio: When the floor opening ratio is set at 40% with a combined opening rate of 40%, the pressure distribution is relatively uniform. For opening ratios between 20% and 60%, the wind speed near the air conditioning side grid outlet is minimal, whereas the wind speed at a distance from the air conditioning side grid outlet is higher. A combined opening approach reduces the wind speed at the far-end floor grille outlet and increases it at the near-end grille and the middle grille of the cabinet channel [13].

(3) Cold and Hot Channel Closure: Closing the cold and hot channels leads to a reduction in the overall temperature within the computer room, enhances uniformity in air distribution, and significantly mitigates the mixing of cold and hot air [8]. This isolation of cold and hot airflows maximizes cold air capacity utilization. The lowest cabinet exhaust air temperature is observed when both cold and hot channels are closed.

(4) Recommendations for Raised Floor Height and Opening Ratio: Increasing the raised floor height from 600 mm to 800 mm reduces the fire loss in the computer room to 10,578.8 kW·K. It is recommended to maintain the raised floor height between 600 mm and 800 mm. At a 40% floor opening rate with combined openings, the entransy loss in the computer room is 8238.3 kW·K, indicating minimal cold and hot air mixing and high cold capacity utilization. When both the cold channel and the combined cold/hot channel are closed, the entransy loss values are 4450 kW·K and 3500 kW·K, respectively. The closure of the cold channel is suitable for computer rooms with air supply below the new floor, while the closure of both cold and hot channels is recommended for computer rooms with high power density and extended air supply distances.

By studying these four influencing factors, it is suggested that the combination of 40% floor grille opening rate and 600–800 mm raised floor height should be used in the actual data center design, and the opening and closing of cold and hot aisles should be used to achieve a better cooling effect in the data center. In this paper, only the airflow organization of the data center computer room with underfloor air supply and closed passage is considered; in addition, the air supply of air conditioning between columns and the air supply of air conditioning on the back panel of the cabinet are also commonly used air conditioning system layout schemes. For other data center rooms in the form of air supply, the simulation optimization of airflow organization needs to be further studied. The simulation accuracy needs to be further improved.

Author Contributions: Conceptualization, J.W.; data curation, J.Z.; writing—review and editing, M.L.; project administration, M.L. All authors have read and agreed to the published version of the manuscript.

Funding: This research was funded by Research and Application of Emergency and Safety Intelligent Management System, grant number 20220111330730018.

Data Availability Statement: The data that support the findings of this study are available from the corresponding author upon reasonable request.

Conflicts of Interest: Author Jingping Zhao, Mengying Li and Jianlin Wu were employed by the company China Academy of Building Research Ltd. The authors declare that the research was conducted in the absence of any commercial or financial relationships that could be construed as a potential conflict of interest.

References

1. Ma, B.; Liu, H.; Du, Y. Simulation and experimental research on the optimization of airflow organization and energy saving in data centers using air deflectors. *Clean Energy Sci. Technol.* **2024**, *2*, 141. [CrossRef]
2. Zhang, Y.; Zhang, K.; Liu, J.; Kosonen, R.; Yuan, X. Airflow uniformity optimization for modular data center based on the constructal T-shaped underfloor air ducts. *Appl. Therm. Eng.* **2019**, *155*, 489–500. [CrossRef]
3. Yuan, X.; Wang, Y.; Liu, J.; Xu, X.; Yuan, X. Experimental and numerical study of airflow distribution optimisation in high-density data centre with flexible baffles. *Build. Environ.* **2018**, *140*, 128–139. [CrossRef]
4. Chu, W.X.; Wang, C.C. A review on airflow management in data centers. *Appl. Energy* **2019**, *240*, 84–119. [CrossRef]
5. Schmidt, R.R. Effect of data center characteristics on data processing equipment inlet Temperatures. In Proceedings of the InterPACK, Kauai, HI, USA, 8–13 July 2001.
6. Patankar, S.V. Airflow and cooling in a data Center. *J. Heat Transf.* **2010**, *132*, 271–291. [CrossRef]
7. Rajagopalan, K.R. Comparative Analysis of Widely Used Air Containment Systems in Commercial Data Centers for Maximum Cooling Performance. Master's Thesis, The University of Texas at Arlington, Arlington, TX, USA, 2013.
8. Gao, C.; Yu, Z.; Wu, J. Investigation of airflow pattern of a typical data center by CFD simulation. *Energy Procedia* **2015**, *78*, 2687–2693. [CrossRef]
9. Cho, J.; Yang, J.; Park, W. Evaluation of air distribution system's airflow performance for cooling energy savings in high-density data centers. *Energy Build.* **2014**, *68*, 270–279. [CrossRef]
10. Schmidt, R.; Vallury, A.; Iyengar, M. Energy savings through hot and cold aisle containment configurations for air cooled servers in data centers. In *ASME 2011 Cacific RIM Technical Conference and Exhibition on Packaging and Integration of Electronic and Photonic Systems*; American Society of Mechanical Engineers: New York, NY, USA, 2011.
11. Shrivastava, S.; Sammakia, B.; Schmidt, R.; Iyengar, M. Comparative analysis of different data center airflow management configurations. In Proceedings of the International Electronic Packaging Technical Conference and Exhibition, San Francisco, CA, USA, 17–22 July 2005; Volume 42002, pp. 329–336.
12. Nakao, M.; Hayama, H.; Nishioka, M. Which cooling air supply system is better for a high heat density room: Underfloor or overhead. In Proceedings of the Thirteenth International Telecommunications Energy Conference-INTELEC 91, Kyoto, Japan, 5–8 November 1991; pp. 393–400.
13. Fulpagare, Y.; Mahamuni, G.; Bhargav, A. Effect of plenum chamber obstructions on data center performance. *Appl. Therm. Eng.* **2015**, *80*, 187–195. [CrossRef]
14. Fakhim, B.; Srinarayana, N.; Behnia, M.; Armfield, S.W. Effect of under-floor blockages and perforated tile openings on the performance of raised-floor data centers. In Proceedings of the 17th Australasian Fluid Mechanics Conference, Auckland, New Zealand, 5–9 December 2010.
15. Schmidt, R.; Karki, K.; Patankar, S. Raised-floor data center: Perforated tile flow rates for various tile layouts. In Proceedings of the Ninth Intersociety Conference on Thermal and Thermomechanical Phenomena in Electronic Systems (IEEE Cat. No. 04CH37543), Las Vegas, NV, USA, 1–4 June 2004; Volume 1, pp. 571–578.
16. Fulpagare, Y.; Hsu, P.H.; Wang, C.C. Experimental analysis of airflow uniformity and energy consumption in data centers. *Appl. Therm. Eng.* **2022**, *209*, 118302. [CrossRef]
17. Sharma, R.; Bash, C.; Patel, C. Dimensionless parameters for evaluation of thermal design and performance of large-scale data centers. In Proceedings of the 8th AIAA/ASME Joint Thermophysics and Heat Transfer Conference, St. Louis, MO, USA, 24–26 June 2002; p. 3091.
18. Herrlin, M.K. Airflow and cooling performance of data centers: Two performance metrics. *ASHRAE Trans.* **2008**, *114*, 182–187.
19. Nada, S.A.; Said, M.A.; Rady, M.A. CFD investigations of data centers' thermal performance for different configurations of CRACs units and aisles separation. *Alex. Eng. J.* **2016**, *55*, 959–971. [CrossRef]
20. Qian, X.; Li, Z.; Li, Z. Entransy and exergy analyses of airflow organization in data centers. *Int. J. Heat Mass Transf.* **2015**, *81*, 252–259. [CrossRef]
21. Iyengar, M.; Schmidt, R.R.; Hamann, H.; VanGilder, J. Comparison between Numerical and Experimental Temperature Distributions in a Small Data Center Test Cell. In Proceedings of the IPACK2007, ASME InterPACK '07, Vancouver, BC, Canada, 8–12 July 2007.

Disclaimer/Publisher's Note: The statements, opinions and data contained in all publications are solely those of the individual author(s) and contributor(s) and not of MDPI and/or the editor(s). MDPI and/or the editor(s) disclaim responsibility for any injury to people or property resulting from any ideas, methods, instructions or products referred to in the content.